

Electronic Supplementary Information (ESI)

‘Hydroelectric Power Plant on a Paper Strip’

Sankha Shuvra Das^a, Shantimoy Kar^{b†}, Tarique Anwar^a, Partha Saha^a and Suman Chakraborty^{ab*}

¹Department of Mechanical Engineering, Indian Institute of Technology Kharagpur, Kharagpur 721302, India.

²Advanced Technology Development Centre, Indian Institute of Technology Kharagpur, Kharagpur 721302, India.

† Currently working as a Postdoctoral Research Associate in Technische Universitat Darmstadt, Germany

email: suman@mech.iitkgp.ernet.in

1. Fabrication details

Whatman filter paper (laboratory grade 1; mean pore diameter $\sim 11\mu\text{m}$ and thickness $\sim 100\mu\text{m}$) are used for our study. Initially, the filter paper was soaked homogeneously in negative photoresist (SU-8 10; MicroChem) for 2-3 minutes. The excess photoresist was squeezed out from the paper to ensure uniform spreading throughout the paper. Thereafter, the photoresist soaked paper was prebaked at 130°C for ~ 10 minutes to evaporate the excess solvent. In the subsequent steps, the paper was cooled to room temperature and exposed under UV radiation ($\lambda \sim 365\text{nm}$) at 100 mW/cm^2 for 20 seconds through a positive mask using mask aligner (OAI Hybralign 2000 series). UV-exposed paper is further post-baked at 130°C for ~ 10 minutes followed by soaking in acetone for ~ 2 minutes (for development) and rinsed in Isopropanol. Finally, the developed channel was dried at $75^\circ\text{--}80^\circ\text{C}$ for ~ 30 minutes.

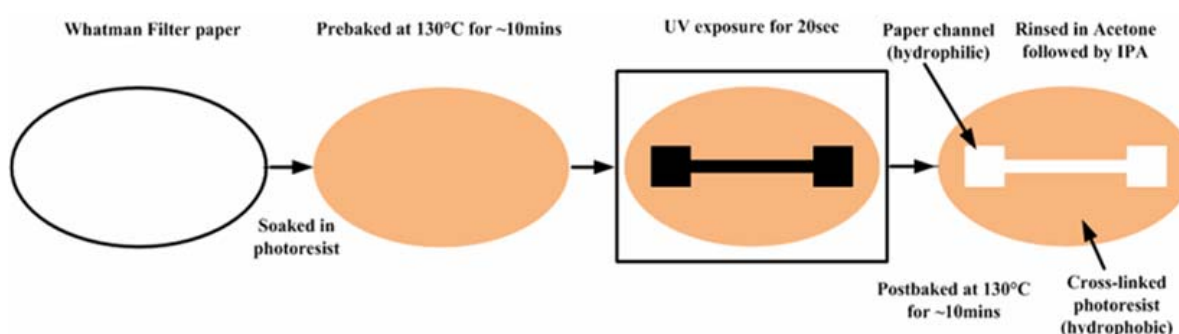


Figure S1: Schematic representation of fabrication of the paper microchannel.

2. Fabrication of pencil-sketched graphite electrodes

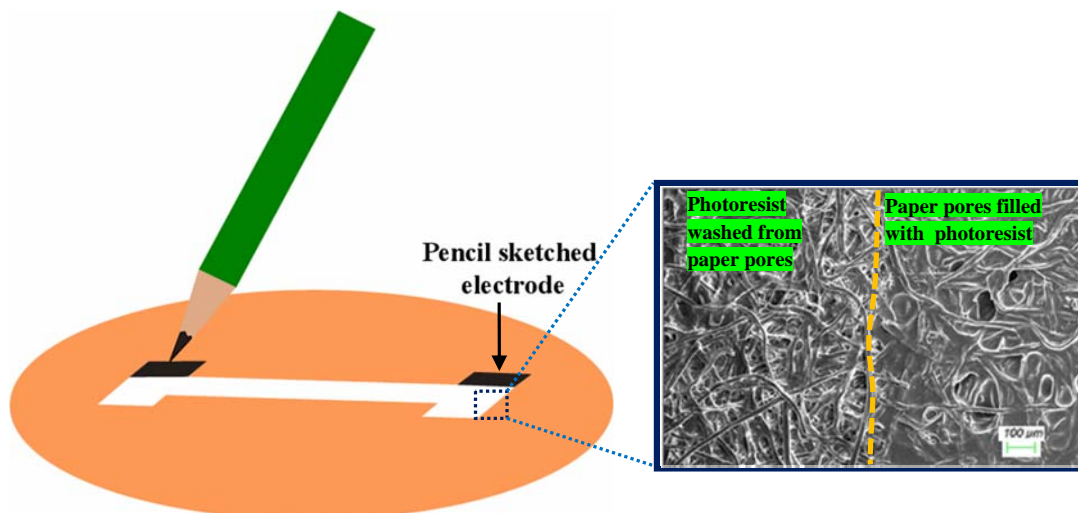


Figure S2: Schematic representation of electrode fabrication (pencil was sketched on front side of the paper surface) and scanning electron micrographs of the fabricated paper device. Half of the reservoir pads were kept free of graphite for the ease of fluid transportation.

3. Effect of electrolyte concentration

The thickness of electrical double layer (EDL) is known to vary with the concentration of electrolyte solution^{1,2}. Therefore, we investigate the effect of electrolyte concentration to explore the effect of EDL on induced streaming potential on the ‘paper-and-pencil’-based platforms.

The induced potential for 10mM and 100mM KCl solution is $\sim -25\text{mV}$ and $\sim -5\text{mV}$ respectively. Thus the induced streaming potential for 10mM and 100mM KCl solution is 4 times and 20 times less than as compared to 1mM KCl solution ($\sim -100\text{mV}$) respectively. Hence, we chose 1mM KCl as the working electrolyte for our experimentations.

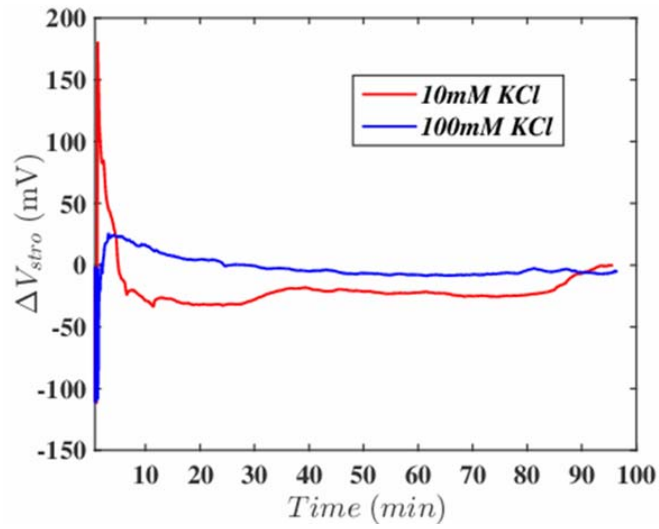


Figure S3: Temporal variation of induced open circuit streaming potential for 10mM and 100mM KCl solution.

4. Streaming potential measurement in different channels

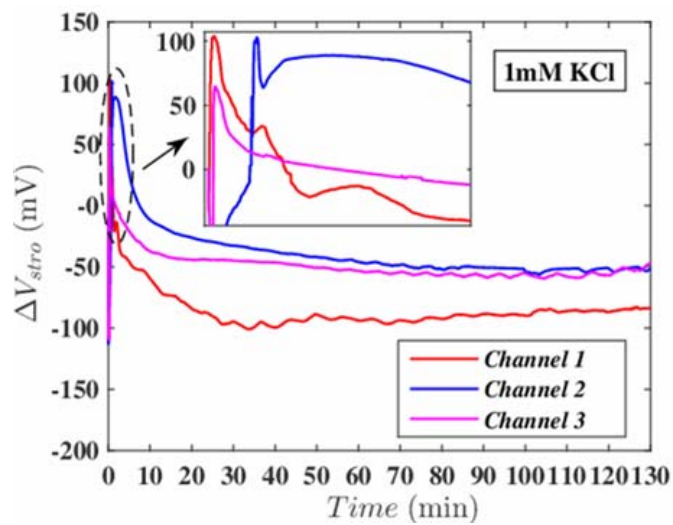


Figure S4: Temporal measurement of open circuit streaming potential for 1mM KCl in **three different channels** of same configuration.

5. Streaming potential (with reverse electrode connection)

In this experiment, the high end of nano-voltmeter probe is connected to the inlet reservoir pad and the low end is connected to outlet reservoir pad.

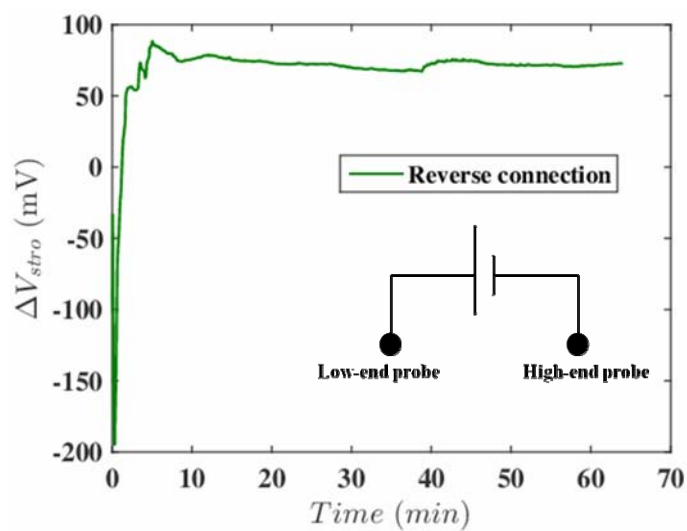


Figure S5: Temporal variation of induced open circuit streaming potential for 1mM KCl in reverse electrode connection mode (inset shows the connection convention).

6. Multichannel microfluidic array

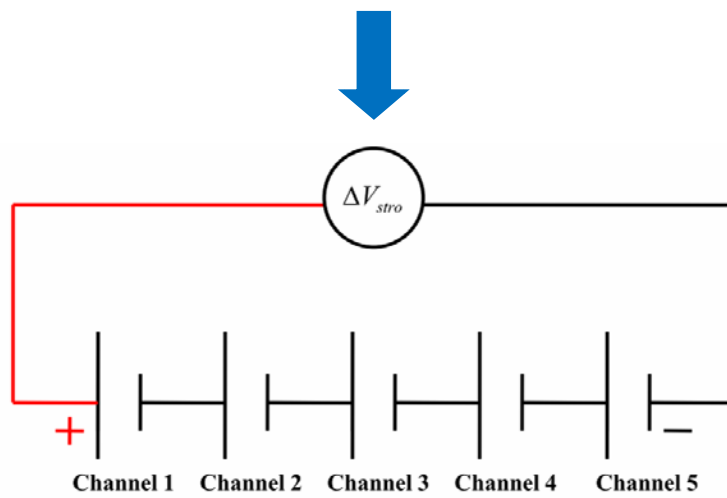
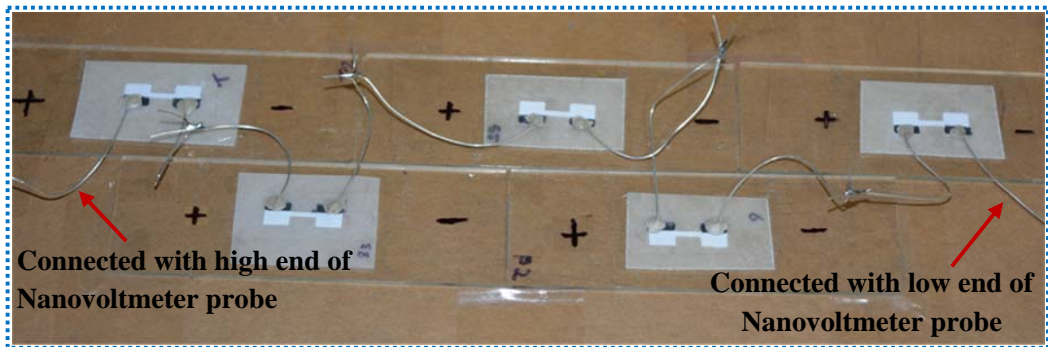


Figure S6: Series connection of multiple channels (for 5 channels).

7. Measurement of device performance against external loads

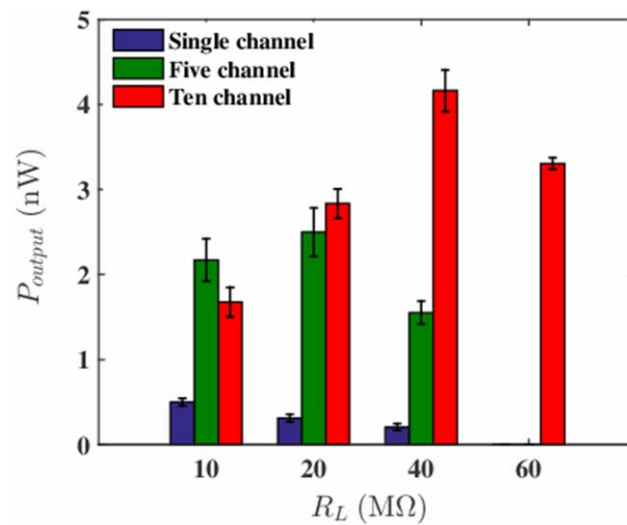


Figure S7: Variation of output power against different load resistance values for different channels.

8. Device performance in different days

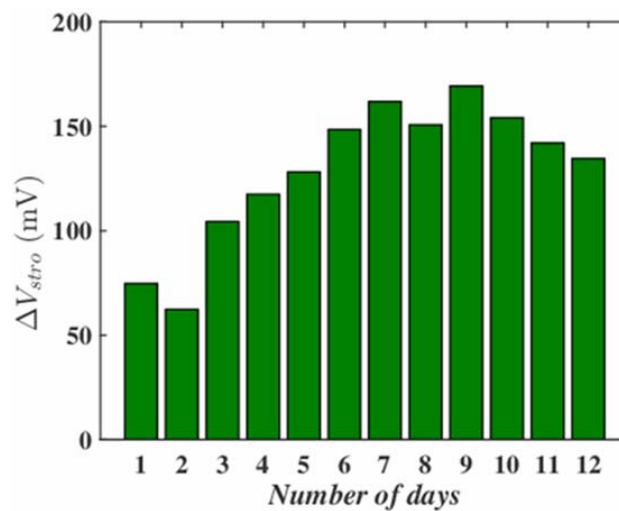


Figure S8: Variation of streaming potential for experiment conducted in different days (for same device with dispensing of electrolyte solution in each ~1 hours; for single channel).

9. Theoretical calculation

In order to build an analytical framework for flows through a complex porous geometrical structure, such as a paper-based channel, here we make some assumptions to simplify the theoretical formalism without sacrificing the underlying physical mechanism of the investigated phenomena. We assume that the porous structure of the paper is constructed of numerous micro-capillaries that are cylindrical in shape having radii R . These capillaries are further assumed to be arranged in parallel. An EDL gets spontaneously developed at the walls of these micro-porous capillaries having a ζ -potential value of ψ_0 .

To obtain the EDL potential distribution (ψ) across a single such channel, we appeal to the Poisson-Boltzmann equation that reads³:

$$\frac{1}{r} \frac{d}{dr} \left(r \frac{d\psi}{dr} \right) = - \frac{ez(n_+ - n_-)}{\epsilon_0 \epsilon_r} = \frac{2ezn_0}{\epsilon_0 \epsilon_r} \sinh \left(\frac{ez\psi}{k_B T} \right) \quad (1)$$

Here, e is the protonic charge, z is the ionic valence (we consider $z:z$ symmetry electrolyte for the analysis), n_{\pm} is the number densities of cations and anions. The number densities are classically expressed through Boltzmann distribution as:

$$n_{\pm} = n_0 \exp(-ez_{\pm}\psi / k_B T) \quad (2)$$

where n_0 is the bulk concentration, k_B is the Boltzmann constant, T denotes the temperature and $\epsilon_0 \epsilon_r$ is permittivity of the medium. For low ζ -potential, typical for such paper-electrolyte systems, we employ Debye–Hückel linearization that recasts Eq. 1 as

$$\frac{1}{r} \frac{d}{dr} \left(r \frac{d\psi}{dr} \right) = \frac{\psi}{\lambda^2} \quad (3)$$

Here, $\lambda = \sqrt{(\epsilon_0 \epsilon_r k_B T / 2n_0 e^2 z^2)}$ is the EDL thickness. This governing equation is complemented with the boundary conditions $\psi = \psi_0$ at the $r = R$ and $\frac{d\psi}{dr} = 0$ at $r = 0$. The system yields a solution of the form:

$$\psi = \psi_0 \frac{I_0(r/\lambda)}{I_0(R/\lambda)} \quad (4)$$

where I_0 refers to the modified Bessel function of first kind of zero order. Now, the electrolyte is transported through the micro-capillary due to a pressure gradient induced by the capillary action of the porous medium. Due to this transport, the total ionic current through a single capillary is given as:

$$I_{ionic} = ez \int (n_+ u_+ - n_- u_-) 2\pi r dr \quad (5)$$

where, u_{\pm} is the velocity of cations and anions, respectively, that may be expressed as:

$$u_{\pm} = u_{str} + u_{cond} = (u_{pressure} + u_{EOF}) \pm \frac{ezE_{str}}{f} \quad (6)$$

Here $f = (e^2 N_A / F \Lambda)$ is the ionic friction factor, N_A is Avogadro's number, F is Faraday's constant, Λ is ionic mobility and μ is the viscosity of the liquid. The ionic mobility may further be represented (using Stokes-Einstein relation⁴) as $\Lambda = (e / 6\pi\mu r_{hs})$ where r_{hs} is the radius of ionic hydration shell. In Eq. 6, the suffices *str*, *cond* and *EOF* denote the streaming, conduction and electroosmotic contributions to the velocity field. Assuming a fully developed flow through a cylindrical capillary, these velocity field contributions read:

$$u_{pressure} = -\frac{1}{4\mu} \frac{dp}{dx} R^2 \left(1 - \frac{r^2}{R^2}\right) \quad (7)$$

$$u_{EOF} = -\frac{\varepsilon_0 \varepsilon_r \psi_0 E_{str}}{\mu} \left(1 - \frac{\psi}{\psi_0}\right) \quad (8)$$

where, $-dp/dx = (2\sigma / RL)$ is the pressure gradient intrinsic to each channel because of capillary effect, σ is the surface tension of liquid and L is the capillary length. Therefore, from equation (6), (7) and (8) we arrive at

$$u_{\pm} = -\frac{1}{4\mu} \frac{dp}{dx} R^2 \left(1 - \frac{r^2}{R^2}\right) - \frac{\varepsilon_0 \varepsilon_r \psi_0 E_{str}}{\mu} \left(1 - \frac{\psi}{\psi_0}\right) \pm \frac{ezE_{str}}{f} \quad (9)$$

Since there is no axially applied electric field, the total ionic current must vanish ($I_{ionic} = 0$)⁵ which leads us to the form of the induced streaming potential given as (from Eq. 5):

$$E_{str} = \frac{\frac{R(ze)^2(\sigma/L)}{\varepsilon_0\varepsilon_r(k_B T)^2} \int_0^R r(1-r^2/R^2)\psi dr}{\frac{\sigma(Rze)^2}{f\varepsilon_0\varepsilon_r(k_B T)} + \frac{(ze)^2\psi_0}{(k_B T)^2} \int_0^R 2\psi\left(1-\frac{\psi}{\psi_0}\right) rdr} = \frac{2ez\sigma R}{\varepsilon_0\varepsilon_r k_B T L} \left(\frac{\frac{ez\psi_0}{k_B T} I_2\left(\frac{R}{\lambda}\right)\left(\frac{\lambda}{R}\right)^2}{I_0\left(\frac{R}{\lambda}\right)} \right) \left(\frac{R^2 e^2 z^2 \mu}{\varepsilon_0 \varepsilon_r k_B T f} + \left(\frac{ez\psi_0}{k_B T}\right)^2 \left(\frac{I_0^2\left(\frac{R}{\lambda}\right)}{I_1^2\left(\frac{R}{\lambda}\right)} - \frac{I_2\left(\frac{R}{\lambda}\right)}{I_0\left(\frac{R}{\lambda}\right)} \right) \right) \quad (10)$$

To calculate the streaming potential, following parameters are used:
 $e = 1.6021 \times 10^{-19} C$, $z = 1$, $R_{hs} = 5 \times 10^{-10} m$ ^{6,7}, $R = 5 \times 10^{-6} m$, $\varepsilon_0 \varepsilon_r = 78.5 \times 8.854 \times 10^{-12} CV^{-1}m^{-1}$,
 $k_B = 1.38 \times 10^{-23} JK^{-1}$, $T = 295 K$, $\sigma = 72 \times 10^{-3} N/m$, $\eta = 0.001 Pa.s$, $L = 5 \times 10^{-3} m$,
 $\psi_0 = -9 \times 10^{-3} V$, $N_A = 6.023 \times 10^{23} mol^{-1}$, $F = 96485.33 C$.

References

- 1 F. H. J. Van Der Heyden, D. Stein and C. Dekker, *Phys. Rev. Lett.*, 2005, **95**, 9–12.
- 2 F. H. J. Van Der Heyden, D. J. Bonthuis, D. Stein, C. Meyer and C. Dekker, *Nano Lett.*, 2007, **7**, 1022–1025.
- 3 S. Das, S. Chanda, J. C. T. Eijkel, N. R. Tas, S. Chakraborty and S. K. Mitra, *Phys. Rev. E - Stat. Nonlinear, Soft Matter Phys.*, DOI:10.1103/PhysRevE.90.043011.
- 4 J. S. Newman and K. E. Thomas-Alyea, *Electrochemical systems*, 2015, vol. 7.
- 5 A. Mansouri, C. Scheuerman, S. Bhattacharjee, D. Y. Kwok and L. W. Kostiuk, *J. Colloid Interface Sci.*, 2005, **292**, 567–580.
- 6 A. Bandopadhyay, J. Dhar and S. Chakraborty, *Phys. Rev. E - Stat. Nonlinear, Soft Matter Phys.*, 2013, **88**, 1–10.
- 7 D. L. Z. Caetano, G. V. Bossa, V. M. de Oliveira, M. A. Brown, S. J. de Carvalho and S. May, *Phys. Chem. Chem. Phys.*, 2016, **18**, 27796–27807.